JOURNAL OF GEOPHYSICAL RESEARCH, VOL. 103, NO. D4, PAGES 3873-3886, FEBRUARY 27, 1998

Estimation of water cloud properties from satellite microwave, infrared and visible measurements in oceanic environments 1. Microwave brightness temperature simulations

Bing Lin

Center for Atmospheric Sciences, Hampton University, Hampton, Virginia

Bruce Wielicki and Patrick Minnis

NASA Langley Research Center, Hampton, Virginia

William Rossow

NASA Goddard Institute for Space Studies, New York

Abstract. Theoretical calculations are used to examine the spectral characteristics of SSM/I (special sensor microwave/imager) brightness temperature (Tb) values for non-precipitating clouds over oceans. It was found that liquid water path (LWP) and the cloud water temperature (Tw) could be derived simultaneously with a technique using the SSM/I 37-GHz and 85-GHz brightness temperatures. Uncertainties in column water vapor (CWV) are the most important error sources in the estimation of LWP and Tw, while ice particles smaller than 100 μm in non-precipitating clouds have a very weak effect (< 1 K) on the Tb values at the relevant SSM/I frequencies. When all SSM/I instrument noise and error sources associated with sea surface temperature, wind speed, and CWV are considered, the biases in LWP from current microwave methods are very small ($\leq$ 0.01 mm) and the standard deviations vary from 0.02 to 0.04 mm. The Tw bias and standard deviation decrease with increasing LWP from about 6 and 8 K, respectively, for clouds with low LWP to < 1 K for LWP > 0.4 mm. For most marine stratocumulus clouds (LWP ~0.1 to 0.2 mm) the Tw bias and standard deviation are about 2 and 4 K, respectively, resulting in cloud height errors of ~1 to 2 km. The method should yield an improvement in the accuracy of retrieved LWP because it more closely approximates cloud temperature than previous techniques. To use the radiative transfer results, it is necessary to normalize or calibrate them to the observations. This relative calibration using 22-GHz brightness temperatures reveals differences of 2.86 K and -1.93 K for the 37-GHz horizontal and 85-GHz vertical channels, respectively, between the SSM/I observations and the model simulations. In multilayered cloud conditions, this new microwave analysis method, when combined with infrared data, should make it possible to determine cloud temperature for an upperlevel ice cloud from the infrared brightness temperatures while simultaneously deriving Tw and LWP for the lower liquid water cloud with the microwave data.

1. Introduction

Quantitative estimates of water cloud properties in marine environments using satellite measurements are critical to the assessment of global climate models. Water clouds not only affect fresh water transport by precipitation, which is one of the key factors determining oceanic thermohaline circulation, but also play a critical role in the radiative energy balance of the Earth/atmosphere system (see *Wielicki et al.* [1995] for a recent summary). The Earth Radiation Budget Experiment (ERBE) [*Ramanathan at al.*, 1989] and the International Satellite Cloud Climatology Project (ISCCP) [*Rossow and Zhang*, 1995] have demonstrated the importance of clouds on the earth's radiation budget at the top of atmosphere and the surface. Changes in cloud vertical distributions and cloud particle phase can affect both shortwave and longwave radiation vertical profiles [*Gupta et al.* 1992; *Wielicki et al.* 1995], the vertical distribution of latent heat release, and cloud feedbacks in a changing climate [*Li and Le Treut*, 1992]. Cloud vertical structure, i.e., cloud layering and overlap, is needed to help diagnose net surface longwave radiation and radiative divergence within the atmosphere from satellite measurements [*Charlock et al.*, 1994]. Thus, monitoring of cloud layering and overlap is a critical component of any climate observing system.

In the tropics, thick anvil clouds cover large areas of the Intertropical and Southern Pacific Convergence Zones (ITCZ and SPCZ). Climatological observations report that about 40% of the clouds are multilayered in these regions [*Poore et al.*, 1995; *Hahn et al.*, 1982, 1984; *Warren et al.*, 1985,1988]. In the midlatitudes, limited ship observations [*Hahn et al.*,

Copyright 1998 by the American Geophysical Union.

Paper number 97JD02816.
0148-0227/98/97JD-02816$09.00

1982] and studies of three-dimensional (3-D) nephanalysis [*Tian and Curry*, 1989] suggest that the frequency of stratus cooccurrence with high clouds is often greater than 50% over oceans. Because low overcast cases block most surface observations and because of the sparse spatial coverage of observational stations, the estimated frequency for multilayered clouds has large uncertainties [*Poore et al.*, 1995]. Satellite observations for multilayered clouds, at present, may be made in cases of thin cirrus over stratus by using infrared (IR) sounder data to determine the upper cloud level and multispectral IR window channel data with spatial coherence methods to determine the lower level clouds [*Baum et al.*, 1994]. Unfortunately, there are almost no methods to estimate other types of multilayered clouds, especially if both layers are optically thick in visible (VIS) and thermal infrared wavelengths [*Wielicki et al.*, 1995].

This paper and its companion [*Lin et al.*, this issue] discuss the estimation of cloud liquid water path (LWP) and temperature (Tw) of nonprecipitating water clouds using combined passive IR, VIS and microwave (MW) satellite measurements. VIS and IR methods are used to discern clear and cloudy sky areas and to retrieve cloud-top temperature and optical thickness [e.g., *Rossow and Lacis*, 1990; *Minnis et al.*, 1993], while the MW technique is used to estimate cloud liquid water path and temperature of water clouds even when they are obscured by high ice clouds.

Satellite MW measurements are commonly used to retrieve LWP over oceans [e.g., *Petty*, 1990; *Greenwald et al.*, 1993; *Liu and Curry*, 1993; *Lin and Rossow*, 1994]. Estimation of cloud water temperatures using passive MW data, however, has only been approached with methods that are basically empirical in nature and involve measurements at lower (< 40 GHz) frequencies [*Pandey et al.*, 1983; *Liu and Curry*, 1993]. Over ocean backgrounds the brightness temperature (Tb) observed from space increases with increasing LWP and cloud height for lower microwave frequencies (see section 3). Thus temperature signals from cloud liquid water can be confused with those from LWP, limiting the use of lower-frequency channels for estimating Tw. Using a microwave radiative transfer model (MWRTM), *Petty* [1990] found that the errors in estimated cloud heights, which are practically interchangeable with cloud temperatures, are about 80 to 100% of cloud height variations if the special sensor microwave/image (SSM/I) data are used alone; that is, cloud height cannot be reliably estimated. In his analysis, however, mean cloud height only varied from about 1 to 2.5 km depending on atmospheric profile, with a standard deviation equal to 60% of the value; that is, the errors of cloud height estimates are around 0.6 to 1.5 km. The potential errors in cloud altitude estimation for higher clouds is unknown.

Furthermore, LWP is generally overestimated when derived with methods that implicitly or explicitly assume a fixed cloud temperature or fixed relationship between Tw and sea surface temperature, and the actual cloud temperature is significantly colder than the assumed value [*Lin and Rossow*, 1994; *Liu and Curry*, 1993]. In the tropics, liquid water marine clouds can range from ~ -40° to almost 25°C. For example, if it is assumed that cloud water temperature Tw is 6°C colder than the surface [*Greenwald et al.*, 1993], midlevel supercooled clouds at -10°C would be ~30°C colder than the assumed cloud temperature over warm tropical seas at 28°C. Thus a method that uses a value of Tw which is closer to the true value for a given retrieval should, on average, lead to more accurate values of LWP.

This paper takes a closer look at the potential for deriving LWP and Tw simultaneously using pairs of both low- (37 GHz) and high- (85 GHz) frequency SSM/I measurements. The primary objective of this study (part 1) is to develop a method for estimating the temperatures of low clouds, provide an improved estimate of LWP, and understand the uncertainties in the retrievals. We will simulate the Tb signatures of SSM/I using a MWRTM and a full range of cloud temperatures (from surface to -40°C), analyze the variations of SSM/I Tb values as functions of LWP and Tw, discuss the sensitivity of microwave retrievals to instrument noise as well as to uncertainties in the major geophysical parameters affecting MW radiation over ocean surfaces, and perform a relative calibration of simulated brightness temperatures to SSM/I satellite observations. The companion paper (part 2) will propose a combined cloud LWP and Tw retrieval scheme based on the MWRTM calculated and calibrated lookup table for SSM/I Tb values, analyze observational LWP and particle size values, discuss the differences between cloud temperatures derived from IR and MW data, and investigate the retrieval of multilayered clouds. By combining MW remote sensing data with VIS and IR measurements in cases of nonprecipitating multilayered clouds, cloud top temperature of the upper ice layer can be measured by using IR measurements, while the field-of-view average cloud temperature and liquid water path of the water cloud beneath the ice can be determined from microwave measurements. This strategy would significantly improve the ability to quantify multilevel clouds over oceans.

2. Simulated Results

To understand SSM/I responses in oceanic environments, we numerically simulate the brightness temperatures of SSM/I at the top of atmosphere (TOA). SSM/I is a seven-channel microwave radiometer that receives microwave radiation at frequencies of 19.35, 22.235, 37.0, and 85.5 GHz (hereinafter referred to as 19, 22, 37, and 85 GHz for brevity). Vertical (v) and horizontal (h) polarization measurements are taken at all frequencies, except at 22 GHz for which SSM/I measures only vertical polarization. The view angle of SSM/I on the Earth is nearly constant at approximately 53°. Although there are theoretical studies on microwave radiation for nonprecipitating clouds [e.g., *Petty and Katsaros*, 1992, 1994], accurate relationships of the response of SSM/I to several geophysical variables are still under study. For example, the variations of brightness temperature with cloud liquid water temperature and liquid water path at 85 GHz are usually not similar to those at lower frequencies.

The model used to simulate SSM/I Tb values is a plane-parallel MWRTM [*Lin and Rossow*, 1997; *Lin*, 1995] which is essentially the same as those of *Wilheit et al.* [1977], *Yeh et al.* [1990], and *Liu and Curry* [1992]. The absorption, scattering, and extinction coefficients and phase functions are calculated according to Mie theory. The complex refractive indices of ice are taken from the tables of *Warren* [1984]. There are basically two available methods to obtain the refractive indices of liquid water droplets: the empirical formulae of *Ray* [1972] and the model of *Liebe et al.* [1991]. For SSM/I frequencies the relative differences of the absorption coefficients of water

Table 1. Cloud Heights for the Four Climate Profiles

	Low	Lower Middle	Upper Middle	High
Tropics	2	4	7	10.5
Midlatitude summer	2	4	7	10.5
Midlatitude winter	2	4	6	7.5
U.S. Standard	2	4	6	8.5

This study only simulates microwave radiation for water clouds with 0.5 km thickness in four different levels: low, lower middle, upper middle, and high as indicated in the table. The units for cloud heights are kilometer.

particles calculated from *Ray* [1972] and from *Liebe et al.* [1991] are generally very small (<5%) when water temperature is above freezing point. For supercooled water, the differences can be large (>15%). It is unknown which one is more realistic because both Ray and Liebe et al. do not have enough measurements to support their modeling efforts for cold (< 0°C) water temperatures. We use empirical formulae of *Ray* [1972] following *Smith et al.* [1992]. The *Liebe* [1985] model and *Petty* [1990] method are employed to specify atmospheric gas absorption and sea surface emissivity, respectively, with a near-sea-surface wind speed (WS) of 7.5 m/s. The atmospheric temperature and gas abundance profiles are taken from climatological profiles for tropical, midlatitude summer, midlatitude winter, and U.S. Standard Atmospheres [*McClatchey et al.*, 1972]. The surface temperatures for these profiles are approximately 26°, 21°, -1°, and 15°C, respectively, and represent a wide range of conditions for ocean backgrounds.

Because the focus is on nonprecipitating clouds, all water droplets are assumed to be smaller than 100 μm. In this case, the dominant microwave radiative process within water clouds is absorption [*Petty*, 1990, and references therein]. For nonprecipitating ice clouds with similarly sized particles, both scattering and absorption are negligible [*Lin and Rossow*, 1996]. Therefore we do not include ice clouds at the present stage and will discuss them later. To illustrate the variability of the LWP and Tw effects on microwave radiances, we use four different liquid water cloud heights in all four atmospheric profiles. These low, lower middle-, upper middle-, and upper level clouds are all assumed to be 0.5 km thick. Thus the liquid water content in each cloud increases with LWP. The corresponding heights for the clouds depend on the atmospheric profiles and are about 2, 4, 6 to 7, and 7.5 to 10.5 km, respectively, as listed in Table 1. The higher clouds represent supercooled liquid water clouds, which have been frequently observed [*Feigelson*, 1978; *Hobbs and Rangno*, 1985; *Sassen et al.*, 1989]. The cloud temperature at upper levels is about -40°C, the expected limit for supercooled water clouds.

The simulated SSM/I responses for low-level clouds (Figure 1), which are similar to those of *Petty* [1990], are shown for the tropics (Figure 1a), midlatitude summer (Figure 1b), midlatitude winter (Figure 1c), and the U.S. Standard Atmosphere (Figure 1d, hereinafter all figures have the same order unless specified otherwise). In clear-sky cases (LWP = 0), all brightness temperatures are very cold (less than 250 K for lower frequencies) due to the low sea surface emissivity of about 0.5 [*Petty*, 1990; *Petty and Katsaros*, 1994]. Vertically polarized brightness temperatures (solid curves) are usually greater than the corresponding horizontally polarized values (broken curves) because sea surface emission is stronger in the vertically polarized direction [*Petty*, 1990; *Petty and Katsaros*, 1994]. The values at 22 GHz (dotted curves) are typically used to estimate column water vapor (CWV), especially in clear-sky cases (compare section 5) because the channel is centered on a weak water vapor absorption line. Thus the following discussion of Tb variations for liquid water clouds concentrates on the other frequencies.

Brightness temperatures at all SSM/I frequencies, especially at 19 and 37 GHz, increase with increasing LWP when it is less than 0.5 kg/m^2 (or 0.5 mm). This nearly linear behavior arises because low-level clouds are physically warmer than the brightness temperatures of the radiance emitted from the surface and atmosphere below the clouds and their total MW absorption optical depths are small. These features serve as the physical basis for using empirical and/or simplified physically based retrieval methods to estimate LWP. Figure 1 also shows that the 37-GHz channels, especially 37h, typically have a stronger dependence of Tb on LWP than the other channels; that is, they are more sensitive to variations in cloud liquid water. On the basis of their sensitivity to LWP, along with a relatively low sensitivity to CWV (see section 4), the 37-GHz channels, especially 37h, are most frequently used to estimate LWP.

The microwave absorption coefficients of liquid water increase with decreasing cloud water temperature, while the cloud physical temperature is usually warmer than the microwave brightness temperature at low frequencies. Thus the brightness temperatures of higher-altitude liquid water clouds (Figure 2) are often greater than the Tb values of lower clouds, especially at 19 and 37 GHz (compare of Figures. 1 and 2). The steeper slope of Tb as a function of LWP in Figure 2 compared to that in Figure 1 clearly reflects that the absorption coefficients of colder clouds are greater than those of warmer ones (see also Figures. 3 and 4). Because both increasing LWP and cloud height can produce greater radiances at 19 and 37 GHz, the signals from cloud liquid water temperature can be confused with those from LWP. These effects limit the use of lower-frequency channels for estimation of cloud temperature [*Lin and Rossow*, 1994, and references therein]. At 85 GHz the situation is different; the Tb values may even decrease with increasing LWP, especially for vertically polarized Tb values (compare Figure 2 with Figure 1). Although the 85-GHz absorption coefficients still increase with decreasing cloud temperature as at lower frequencies, the sign of the change in Tb with LWP depends on the competition between cloud temperature and upwelling microwave radiation at cloud base. The absorption coefficients only affect the rate of change of Tb values with LWP, not the sign.

To determine the variation of MW radiation with cloud water temperature, we examine the Tb results for all four cloud height cases. Figure 3 shows the horizontally polarized 19- and 37-GHz brightness temperatures at the top of the atmosphere (TOA). Vertically polarized Tb values (not shown) have similar features. As expected, the Tb values at both frequencies increase as LWP and cloud height increase. The range in Tb differences between the various cloud levels is greater for the warmer atmospheres than for the colder profiles

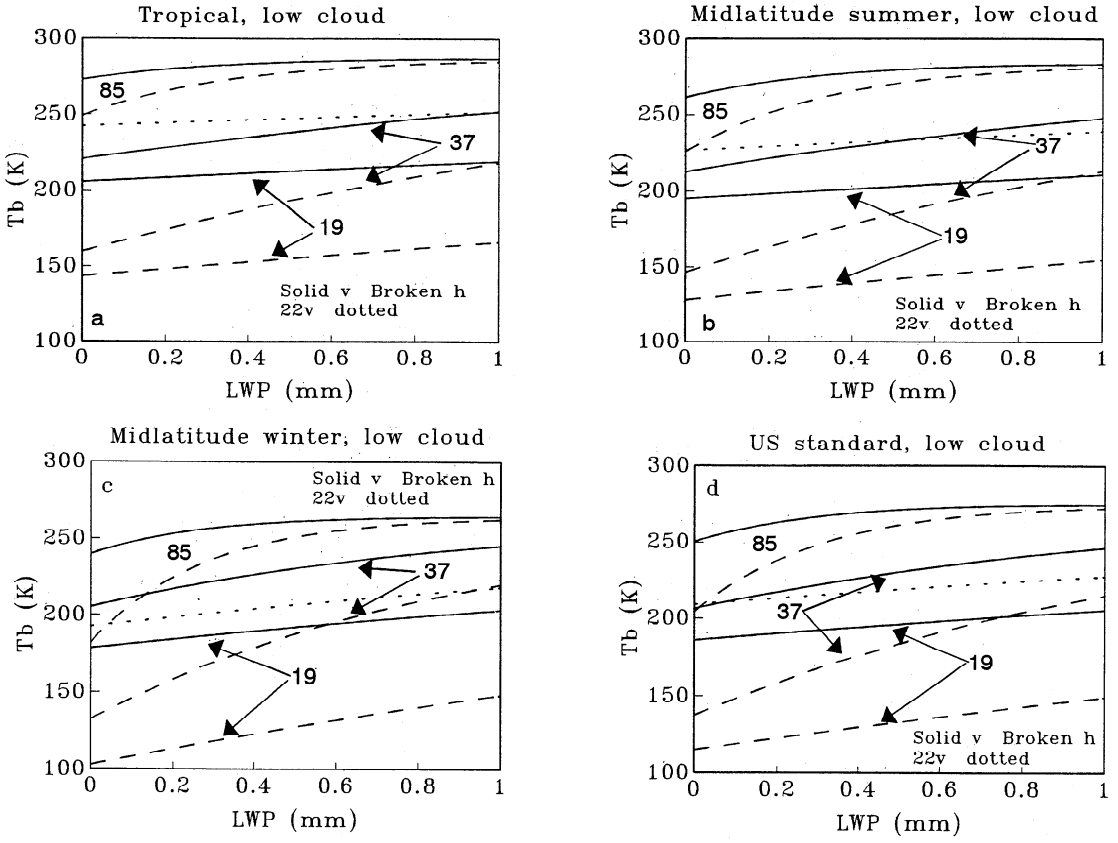

Figure 1. Simulated SSM/I (special sensor microwave/imager) brightness temperatures for low level liquid water clouds in the tropical (top left; a), midlatitude summer (top right; b), midlatitude winter (bottom left; c), and US standard (bottom right; d) atmospheric environments. The dotted curve is for 22v. The other six curves represent the remaining SSM/I vertically (solid curves) and horizontally (broken curves) polarized Tb values. The units for brightness temperatures and LWP values are K and mm (or kg/m^2), respectively.

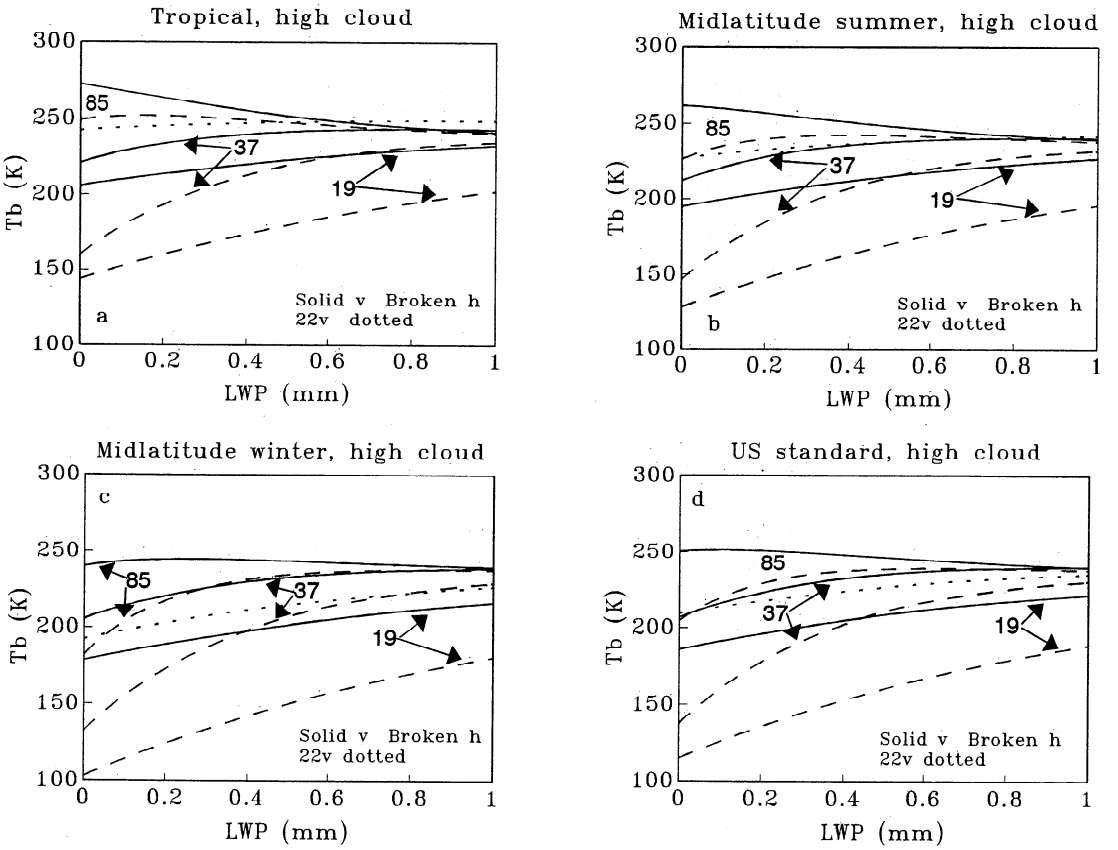

Figure 2. Same as Figure 1 except for high-level liquid water clouds.

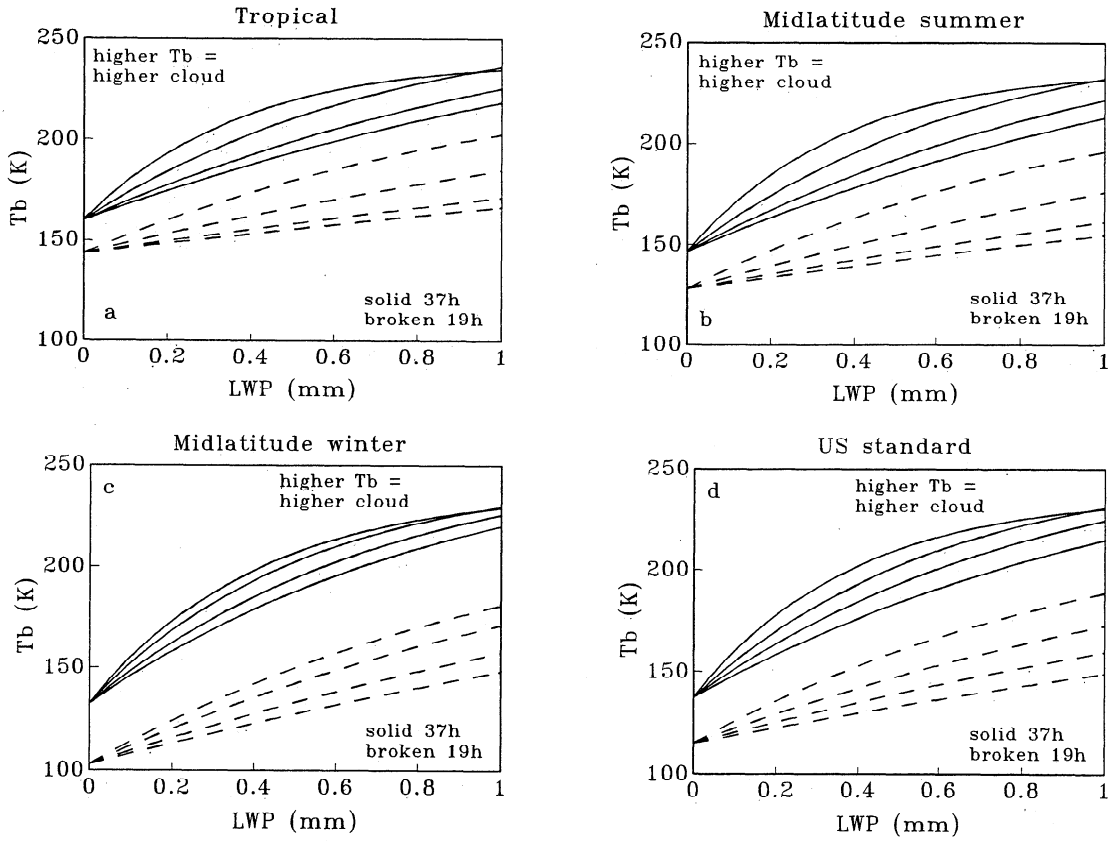

Figure 3. Simulated horizontally polarized brightness temperatures of SSM/I at 37 (solid curves) and 19 (broken curves) GHz for various atmospheres. The four curves for each frequency represent Tb for high, upper-middle, lower-middle, and low-level liquid water clouds. Tb increases with increasing altitude. As in Figure 1, the four panels are for the four atmospheric environments.

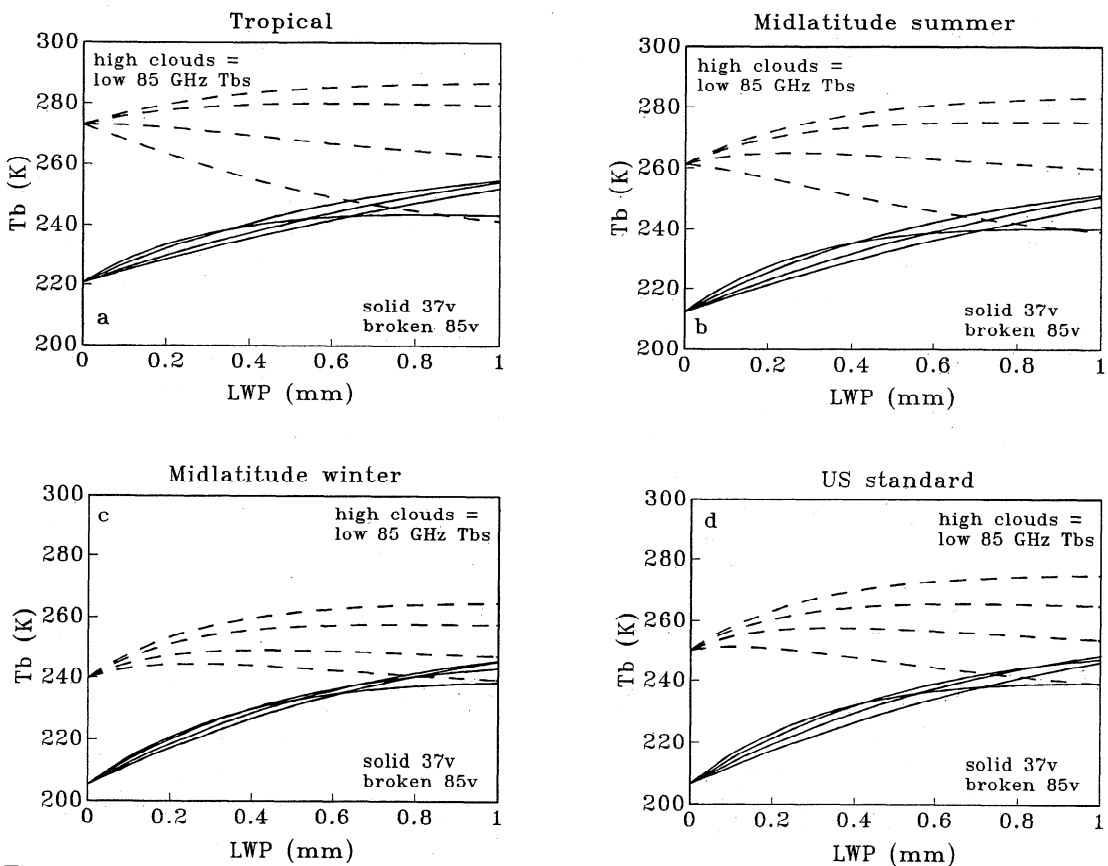

Figure 4. Same as Figure 3 but for 85 (broken) and 37 (solid) vertically polarized Tb values. For 85 GHz, Tb decreases with increasing altitude.

primarily because of the larger potential range in Tw in warmer climates (i.e., there are larger temperature differences from the surface to about -40°C in warmer climates than for colder climates). For a given Tb at either 19 or 37 GHz, there are multiple solutions for LWP as a function of varying cloud temperature (or height). Furthermore, the LWP errors produced by incorrectly accounting for Tw in one channel, say *37h*, cannot be determined with the other channel. The variations of Tb with LWP and Tw in these two channels are very similar, especially when LWP is less than about 0.5 mm, a range that includes most nonprecipitating clouds. Thus it is impractical to estimate cloud temperature using only the lower-frequency channels [*Lin and Rossow*, 1994, and references therein].

Figure 4 shows the vertically polarized Tb values at 37 and 85 GHz for the same conditions used in Figure 3. By comparing to Figure 3, it is clear that the Tb_{37v} values have features similar to Tb_{37h} except that the Tb_{37v} values are larger, much less sensitive to Tw, and somewhat less sensitive to LWP than Tb_{37h}. Unlike the lower-frequency Tb values, Tb_{85v} may increase or decrease with increasing LWP depending on the difference between Tw and brightness temperature from emission below the clouds, as mentioned earlier. Moreover, for the same LWP, Tb_{85v} for all four climatic profiles decreases with increasing cloud height; that is, the higher the clouds the colder the brightness temperatures. Comparing the values of Tw - Tb between warmer and colder clouds, we find that the values are small or even negative in colder clouds, and the changes in liquid water absorption coefficients at 85 GHz as a function of cloud temperature only affect the relative magnitude of the Tb changes. Thus in the competition between the effects of changing water absorption coefficient and cloud temperature on TOA brightness temperature, the latter dominates. These two factors (the temperature difference and water absorption coefficient) enhance the depression of Tb_{85v} when Tw - Tb is less than zero, or when the clouds are very cold (compare of Figure 4). This result demonstrates that the dependence of Tb_{85v} on Tw has a sign opposite that for the lower frequencies.

As a result, we propose to estimate LWP and Tw simultaneously using SSM/I measurements at 37 and 85 GHz. We use the observed Tb values at 37 and 85 GHz as input for our calculated SSM/I Tb lookup table and then search for the best match between the observed and the simulated Tb values to obtain simultaneous estimates of LWP and Tw. Because most clouds are not optically thick at these wavelengths, Tw represents a liquid-water-content-weighted temperature averaged over the water cloud layer. The detailed retrieval scheme is discussed in part 2 of this series of papers [*Lin et al.*, this issue]. This method generally can be used for single-layered, nonprecipitating water clouds. For multilayered, nonprecipitating water clouds, because Tw values are the averages for water cloud layers, the cloud height estimates can be different from the real clouds. The *85h* Tb values (not shown here) are similar to those at *85v* Tb values except that they do not depend so strongly on LWP and Tw for the coldest clouds.

The decrease in Tb with increasing cloud height at 85 GHz is similar to brightness temperature variations at thermal IR wavelengths. There are several differences, however, between thermal 85-GHz microwave and IR radiation.

1. The Tb values at thermal IR wavelengths are usually determined by cloud-top temperature and are relatively insensitive to LWP, since most water clouds have emissivity near 1 (LWP > 0.05 mm). For thermal radiation at 85 GHz the optical thickness for the majority of nonprecipitating clouds (LWP < 0.5 mm) is less than 1 [*Petty and Katsaros*, 1992]; that is, the Tb values at TOA are strongly affected, not only by Tw but also by LWP, CWV, sea surface temperatures (SST), and WS.

2. Thermal IR Tb values typically decrease monotonically with increasing cloud height and LWP if clouds are very thin. The 85-GHz Tb values may increase or decrease with LWP depending on both Tw and Tb, which varies strongly with CWV and surface emissivity.

3. Thermal IR Tb values are very sensitive to ice cloud, while nonprecipitating ice cloud has very little effect on MW radiation, especially at the SSM/I frequencies as demonstrated in the following section:

The first two differences listed above indicate that cloud temperatures estimated at IR wavelengths will more closely approximate cloud-top temperature, while Tw estimated at microwave wavelengths will more closely approximate a layer average cloud temperature. The third difference suggests that the MW measurements can be used to estimate the height of a liquid water cloud layer beneath a cirrus layer, even if the cirrus layer were optically thick in the thermal IR. In this manner the IR data could be used to determine cloud-top temperature (or altitude) of the upper cloud layer, while the MW data determine the height of the liquid-water cloud beneath the cirrus.

3. Sensitivity Test

To understand the effects of geophysical parameters on microwave radiation and to predict the accuracy of any resulting LWP and Tw retrievals, we simulate the SSM/I Tb uncertainties associated with the potential errors in sea surface temperature, wind speed, column water vapor, and scattering by ice particles. *Lin and Rossow* [1994] examined a similar problem using a simplified microwave radiative transfer method. In their results, they concentrated on lower frequencies using observed SSM/I data. Here we will extend those results to include the SSM/I high-frequency channels and to theoretically investigate the effects of ice scattering. We first focus on the Tb sensitivities of low and lower middle-level clouds since many water clouds are below about 4 km, then provide an error analysis on LWP and Tw estimates in terms of multichannel and multidimensional error dependencies.

The theoretical calculations show that for the lower middle-level clouds in a midlatitude summer climatological profile, the changes of the Tb_{37v} and Tb_{37h} change with LWP by about 0.5 K and 1 K per 0.01 mm, respectively. The lower sensitivity of the vertical polarization results from the smaller temperature differences between the cloud water and the microwave radiation (i.e., $|Tw - Tb_{37v}| < |Tw - Tb_{37h}|$). At 85 GHz, the v and h Tb vary with cloud temperature by about 1.4 K and 1 K per 1 °C per 1 mm, respectively. The larger the LWP, the greater the sensitivity of Tb to changes in Tw (compare of Figure 4). The total errors in microwave-estimated LWP and cloud temperature are primarily caused by the SSM/I

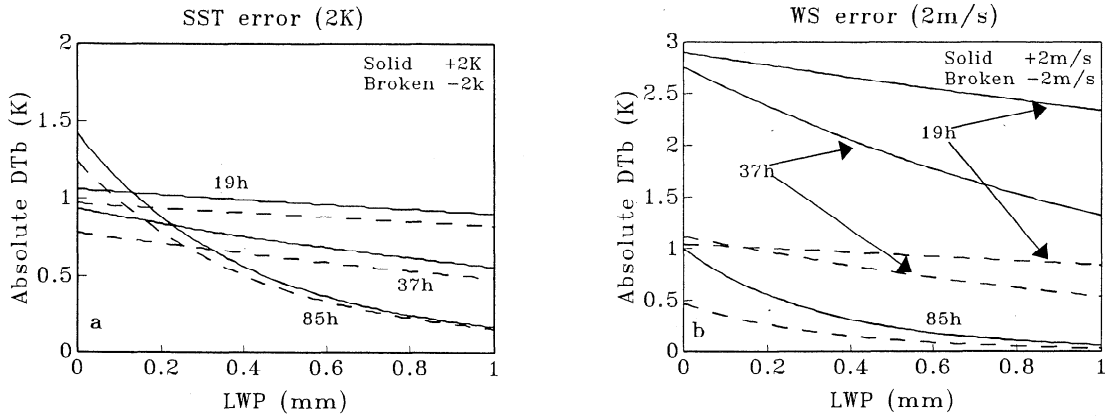

Figure 5. Simulated absolute values of uncertainties of 19, 37, and 85 GHz horizontally polarized brightness temperatures due to errors of ±2 K sea surface temperature (a) and ±2 m/s near sea surface wind speed (b) for lower-middle level clouds in the midlatitude summer profile.

multichannel noise and uncertainties in the retrieval inputs (such as CWV, WS, and SST).

To provide sensitivity tests of individual error sources, all geophysical parameters, except the parameter being tested, used in the microwave radiative transfer model are fixed at the values discussed in the previous section. We then determine the TOA brightness temperature errors that would result from an uncertainty in the tested parameter. Because of the similarity between vertical and horizontal brightness temperatures the results are only shown for the horizontal polarization case.

Figure 5 shows the absolute value of the Tb error caused by an error DTb of ± 2K in SST (Figure 5a) and by an error of ±2 m/s in the near-surface wind speed (Figure 5b). Results are given for the midlatitude summer climatological profile. The assumed errors in SST and WS are representative of current remote sensing algorithm accuracies [*Rossow and Garder*, 1993; *Goodberlet et al.*, 1990].

Figure 5a shows that the Tb uncertainties in caused by 2K errors in SST are usually less than 1K, the level of SSM/I instrument noise. Given the sensitivity of LWP to Tb, this result indicates that SST errors are a minor source of error for determination of LWP or Tw. For the uncertainties in WS the Tb values at 85 GHz are within the instrument noise level, but the Tb values at lower frequencies are in error by 2 - 3 K, which is significant for LWP estimation. The unequal absolute value of DTb between the +2 m/s WS and -2 m/s WS errors shown in Figure 5b are produced by the nonlinear relationship between sea surface emissivity and near-surface wind speed. Since the climatological near-surface wind speeds are about 3 to 10 m/s, this nonlinear behavior will cause a bias in retrieved LWP even if WS errors are random and unbiased [*Lin and Rossow*, 1994].

The effect of errors in CWV for all four climatological atmospheric profiles are shown in Figure 6. CWV errors are assumed to be ±10%. Given 10% relative error, the absolute CWV error in the tropics and the summer midlatitudes is about 3 - 4 kg/m^2, which is the current level of uncertainty for microwave remote sensing of CWV [*Sheu and Liu*, 1995]. Other studies [e.g., *Petty*, 1990] have claimed much smaller (about 1.5 - 2 kg/m^2) errors in estimated CWV. As shown in Figure 6, the resulting Tb errors (about 3 K or larger at 19 and 37 GHz) are significantly greater than those found for SST or WS. An exception occurs for the midlatitude winter profile which has a small CWV amount (about 8.5 kg/m^2) and therefore much smaller absolute errors in CWV. The errors at 85 GHz rapidly decrease with increasing LWP because liquid water absorption and emission are much stronger at 85 GHz than at the lower frequencies. Figure 6 indicates that the uncertainties in CWV are the most important source of error in estimating LWP, especially at lower frequencies, as discussed by *Lin and Rossow* [1994]. The 37-GHz channels show less sensitivity to CWV errors than 19 GHz for all values of LWP and are less sensitive than 85 GHz for small values of LWP. This is one of the reasons for using the 37 GHz Tb values to estimate LWP. If the CWV errors at 37 GHz are converted to equivalent errors in retrieved LWP, the resulting uncertainty in LWP is about 0.05 mm, similar to the values given by *Lin and Rossow* [1994]. More accurate CWV values are required not only for studies of water vapor but also for methods that utilize passive microwave radiances to estimate cloud LWP. While the current approach is different, the above sensitivities to SST, WS, and CWV are consistent with those from *Lin and Rossow* [1994]. For LWP < 0.2 mm, the errors (about 3 to 7 K) at 85 GHz caused by CWV uncertainties are much larger than SSM/I instrument noise. These errors may cause large errors in cloud water temperature estimates if only the 85-GHz channel is used in the retrieval. When LWP and Tw are estimated simultaneously, most Tb errors caused by CWV are canceled by similar Tb errors in LWP estimates using 37 GHz. Thus the errors in Tw estimates are reduced (see results below and compare Figures 9 and 10).

To consider the effect of ice clouds on microwave radiation, we place an ice cloud layer above the top of a lower middle-level liquid water cloud layer. The two-layer cloud cases use the summer midlatitude climatological profile. Results for other water cloud levels and climatological profiles are similar. Figure 7 shows the effects of ice scattering on TOA Tb changes for ice clouds composed of 40-μm radius spheres (Figure 7a) and 100-μm spheres (Figure 7b). Brightness temperature changes are small at all frequencies (less than 1 K), even for extremely thick ice clouds (IWP = 0.6 and 0.9 mm). In general, the effect of the ice-cloud layer increases with frequency and with particle size. Ice absorption at MW

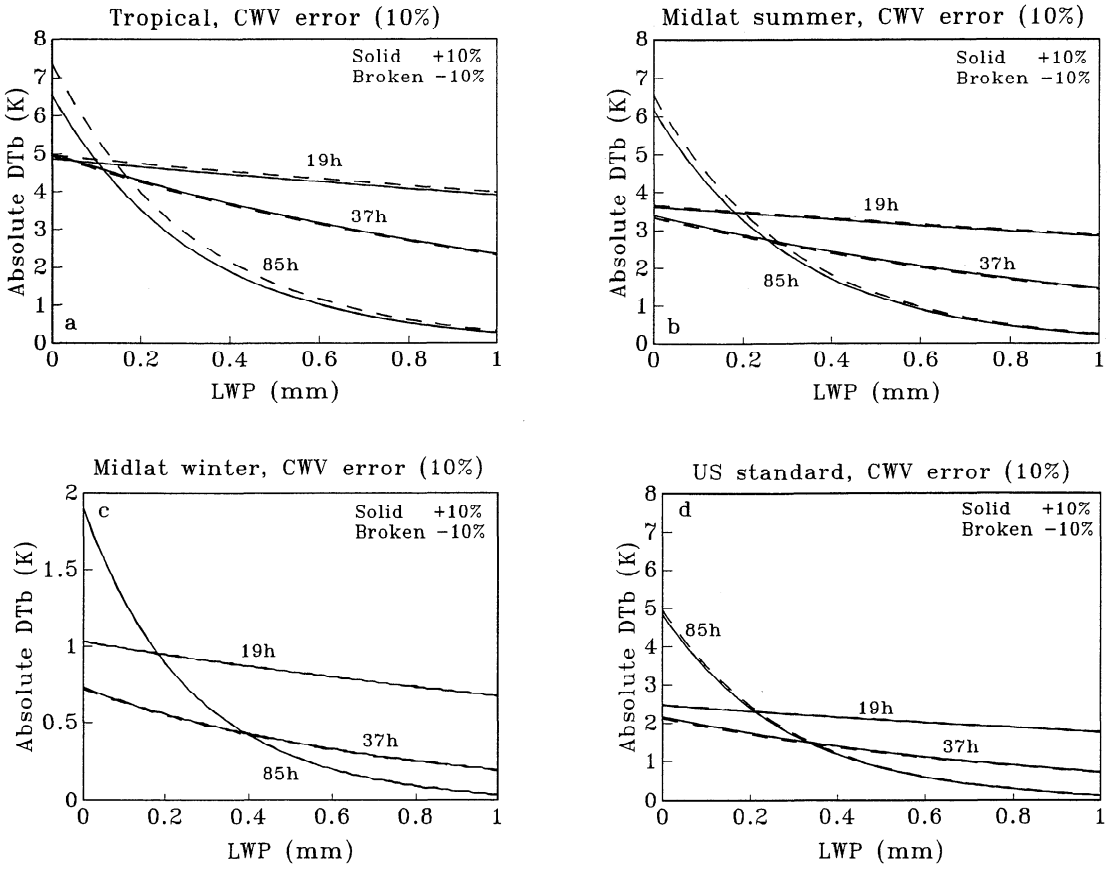

Figure 6. Same as Figure 5, but with ± 10% CWV uncertainties for the four atmospheric environments.

wavelengths is very low due to the minimal imaginary part of the refractive index for ice [*Warren*, 1984]. The scattering effects of small ice particles (radius less than 100 μm) are also negligible because the particle size parameter is much less than 1, even at 85 GHz. Thus nonprecipitating ice clouds usually are not detected by current microwave instruments [*Lin and Rossow*, 1996]. With increasing ice crystal size, scattering effects become more important, especially at 85 GHz.

Figure 8 gives results for 500-μm radius ice particles for the same conditions used in Figure 7. In this case, the scattering effects are large at 85 GHz (Figure 8c). Ice-scattering effects at 85 GHz depend strongly on IWP (10 to 30 K) and less on the upward emission of microwave radiation by the sea surface and liquid cloud layer below (hence the dependence on LWP shown in Figure 8c). The effect of ice scattering is small at 37 GHz for most liquid water clouds (Figure 8b, less than 1K for LWP < 0.5 mm) and probably undetectable at 19 GHz (Figure 8a; notice the scale differences among the three panels). The reduced scattering effects at 37 and 19 GHz are caused by the decreasing particle size parameter at the lower frequencies.

The above sensitivity tests suggest that most

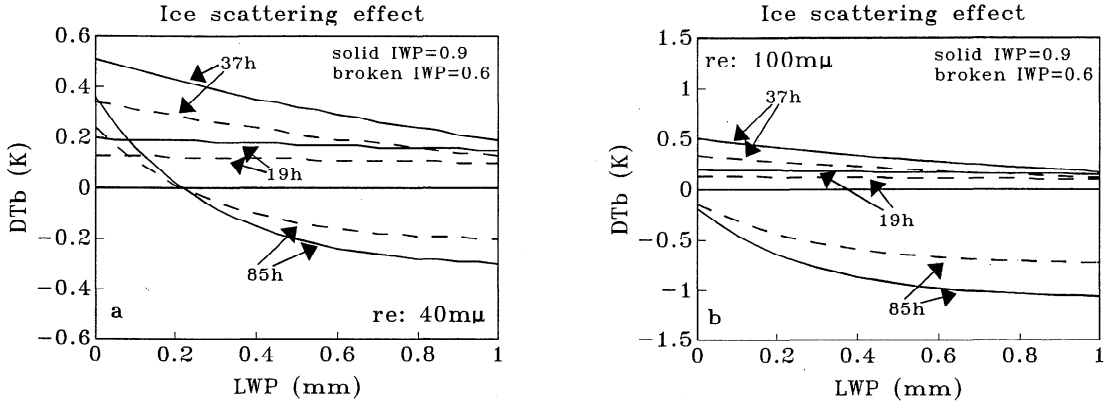

Figure 7. Simulated horizontally polarized brightness temperature variations at 19, 37, and 85 GHz associated with (a) 40- and (b) 100-μm radius ice particles. Broken and solid curves are for IWP = 0.6 and 0.9 mm, respectively.

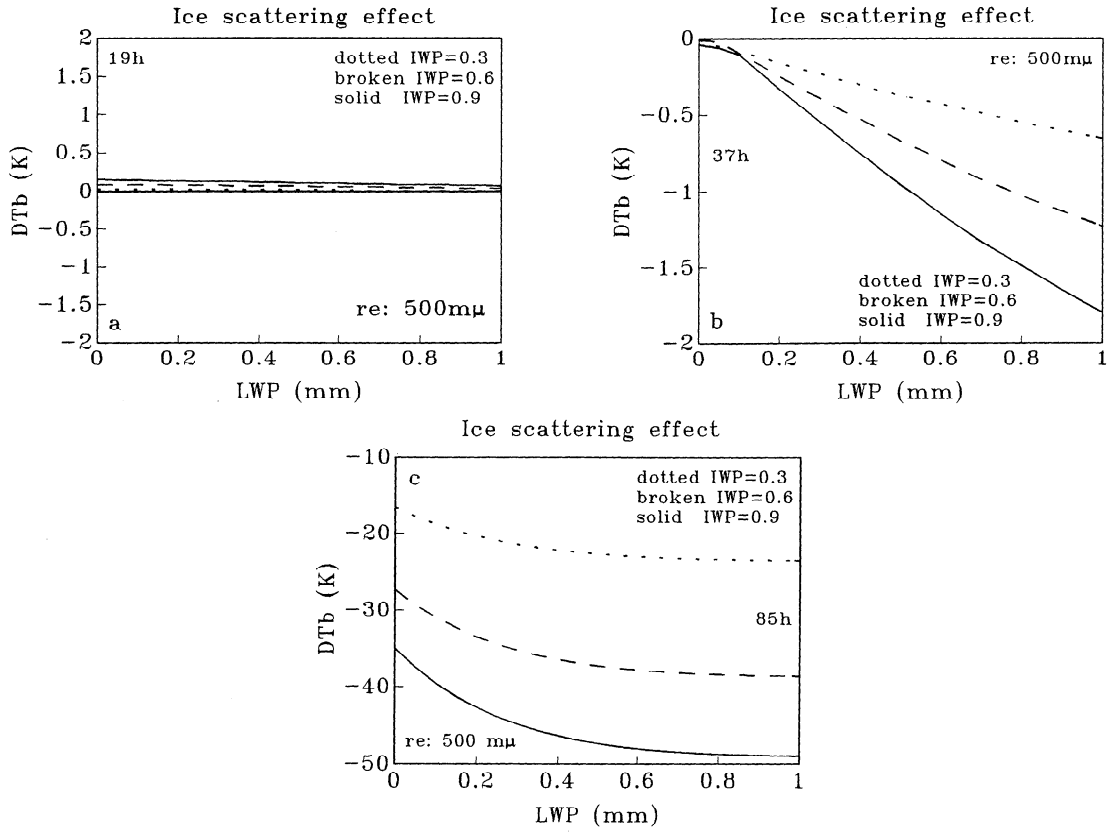

Figure 8. Same as Figure 7 but with 500-μm radius ice particles for 19 (a), 37 (b), and 85 (c) GHz, respectively. Dotted, broken and solid curves are for IWP = 0.3, 0.6 and 0.9 mm, respectively.

nonprecipitating ice clouds have minimal effect at 19 through 85 GHz. As a result, by combining IR and MW satellite measurements, we can expect to estimate the temperatures of both an overlapped ice cloud layer (using IR) and water cloud layer (using MW) with reasonable accuracy for most cases of overlapped cloud over ocean. Exceptions include ice clouds with both very large particles and large IWP, or cases of very low LWP (< about 0.04 mm; see discussions later).

To test LWP and Tw estimates for microwave methods in terms of multichannel and multidimensional error dependencies, we simulate the complete microwave retrieval processes. Because ice clouds have very weak effects on microwave radiation, the following simulation assumes IWP = 0. The actual simulation procedure is as follows: (1) For a given climatological profile, obtain initial values of SST_0, WS_0, CWV_0, LWP_0, and Tw_0; (2) calculate brightness temperatures at TOA using MWRTM for each relevant channel; (3) add instrument noise to the calculated brightness temperatures to simulate SSM/I Tb values; (4) add errors to the original values of SST_0, WS_0, and CWV_0 to obtain simulated inputs of SST, WS, and CWV; (5) retrieve LWP and Tw values using SST, WS, and CWV from step 4 and Tb values from step 3; (6) repeat steps 3 to 5 100 times for each value of LWP_0 and Tw_0 in order to have enough data for stable statistics. Here, we assume all error sources are Gaussian random variables. The SSM/I instrument noise levels obtained by *Hollinger et al.* [1990] are used as the standard deviation (or σ) in the simulation. Because of field of view (FOV) differences between 85 GHz and other channels (four to one), averaged Tb values at 85 GHz are used for each pixel at lower frequencies. Because the size of marine stratiform clouds is generally > 5 km [*Tian and Curry*, 1989; *Liao et al.*, 1995] and adjacer clouds tend to locate in the same level, the effect of th remaining FOV differences between 37 and 85 GHz on LW and Tw retrievals is minimal for these clouds. For broke clouds this effect produces random errors that can be small the averages. As discussed before, the errors in SST and W are 2 K and 2 m/s, respectively. Because CWV is the mc important error source (Figure 6 or *Lin and Rossow* [1994 we use averaged CWV retrievals to reduce random errors. Th study and its companion use an average of four adjacent CW values as input to estimate LWP and Tw values. If it assumed that the uncertainties in the four values of CWV us in the pixel averaging are uncorrelated, then it can concluded that the errors in CWV are about half of t uncertainties discussed earlier (i.e., 5%). Although t assumption may not be valid in all cases, it yields a CV uncertainty comparable to that given by *Petty* [1990] CWV.

While the details of the LWP and Tw retrieval scheme discussed in the companion paper, a brief overview is gi here. IR and MW remote sensing measurements are the prin inputs for the retrieval algorithm. SST and cloud temperature are estimated from IR measurements, while WS CWV are MW retrievals. For a given set of these parame and the SSM/I Tb values (here all Tb values are simul values with Gaussian instrument noise) the sch automatically searches for the best solution from cloud down to the surface according to a MWRTM-produced loc table. Because of monotonic functions of Tb37 and Tb8

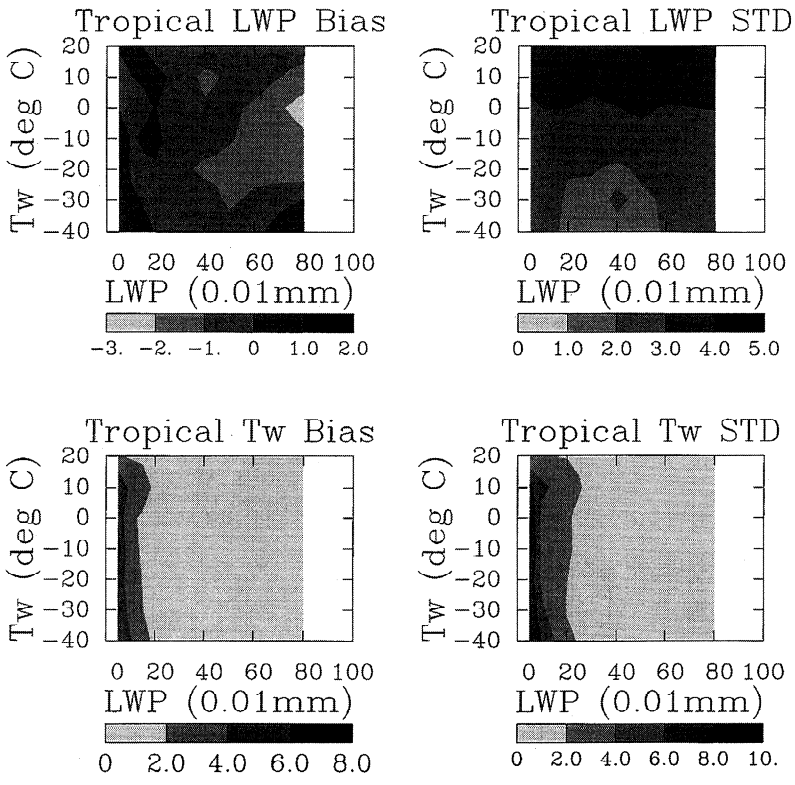

Figure 9. Simulated bias (left) and standard deviation (right) of LWP (top panels, in units of 0.01mm or mg/cm^2) and Tw (bottom panels, in units of °C) for tropical climates.

LWP and Tw (compare Figures 3 and 4) the current method has unique solution.

Figures 9 and 10 are the simulated results of LWP and Tw biases and standard deviations for the tropical and midlatitude winter profiles, respectively, which represent the extreme conditions in this analysis. The patterns of the parameter bias and standard deviation in both figures are more or less similar. However, the magnitudes of the errors for midlatitude winter are much smaller because of the reduced absolute CWV uncertainties. Thus, we will focus on the worst case scenarios exemplified in the tropical results.

In Figure 9, the LWP biases (top left panel of Figure 9) are mostly within $\pm$0.01 mm of the reference values, especially for LWP less than 0.5 mm (i.e., for most nonprecipitating clouds). The standard deviation of the LWP error (top right panel of Figure 9) decreases from about 0.04 mm for warm clouds to about 0.02 mm for cold clouds due to the temperature dependence of liquid water absorption.

The bias and standard deviation of Tw errors (bottom panels of Figure 9) decrease with increasing LWP from values of about 6 and 8 K, respectively, to < 1 K. For most marine stratocumulus clouds (LWP about 0.1 - 0.2 mm), bias error is about 2 K with standard deviation about 4 K, which is basically consistent with the estimate from *Petty* [1990]. When cloud LWP increases, radiation emitted from clouds at 85 GHz dominates over that from the surface and from the atmospheric gases. As a result, the error in Tw decreases with increasing LWP. This result suggests that the uncertainty in microwave-estimated cloud height is about 1-2 km for most liquid water clouds.

Current retrieval technique should obtain more accurate LWP values than those estimated from the methods that implicitly or explicitly assume a fixed cloud water temperature or fixed relationship between Tw and SST when the actual cloud water temperature is considerably colder than the assumed value. Figure 11 shows the simulated bias and standard deviation values of LWP estimates for tropical (top panels) and midlatitude winter (bottom panels) profiles. All simulating processes are the same as those done for Figures 9 and 10 except using a cloud water temperature equal to SST-6 [*Greenwald et al.*, 1993] during retrieving LWP. Although the LWP standard deviations in Figure 11 are only slightly larger than those in Figures 9 and 10, the bias errors (all positive) are much larger (note the scale difference between Figure 11 and Figures 9 and 10), especially for tropical cases. For example, the errors can be as large as about 0.15 mm for a tropical cloud with LWP = 0.1~ 0.2 mm and Tw = -10°C. Even for tropical warm clouds the biases could be about a factor of 2 larger. Also, the thicker the clouds the bigger the positive biases because, generally, the LWP errors caused by Tw errors are proportional to the products of the relative errors of cloud absorption coefficients (which can be 100% for a temperature range from -20° to 20°C, compare *Liu* and *Curry* [1993]) and LWP values. These results illustrate that the combined retrieval of LWP and Tw may reduce the errors in LWP by about a factor of 2 because it could yield a temperature that is closer to the true cloud temperature than assumed in most microwave LWP retrievals.

4. Calibration

To use the model-simulated results to estimate geophysical parameters (LWP and Tw), we need to calibrate the radiative model Tb values to be consistent with SSM/I measurements.

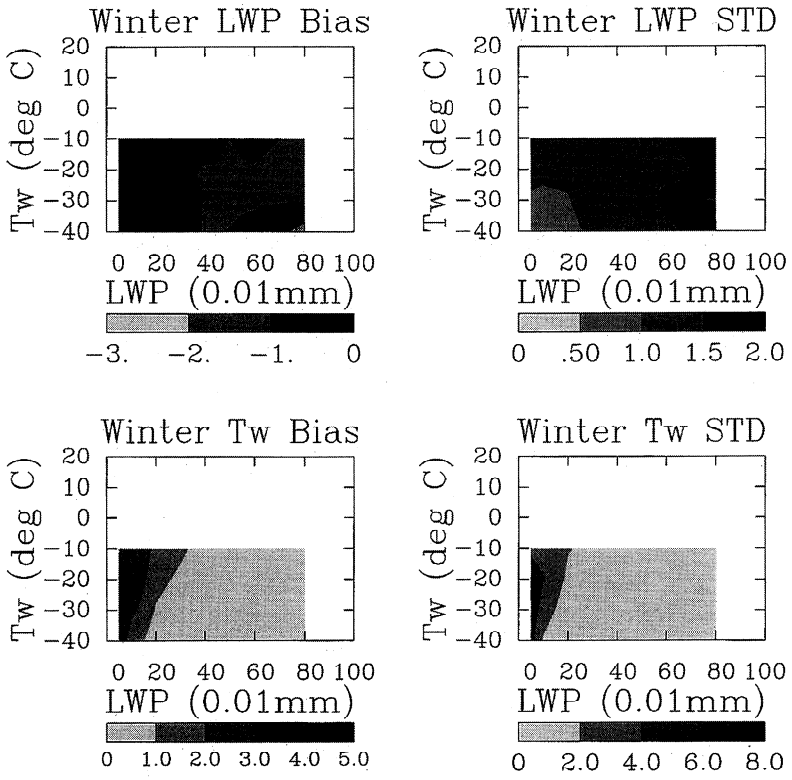

Figure 10. Same as Figure 9 but for midlatitude winter climates.

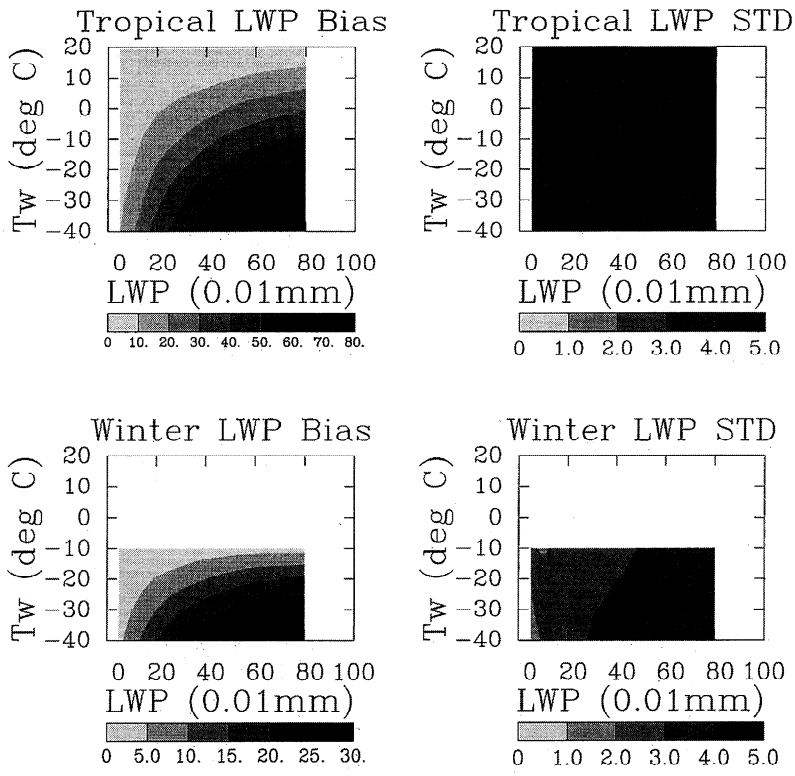

Figure 11. Same as Figures 9 and 10 but for the bias and standard deviation of LWP values estimated from the method assuming Tw = SST-6 for tropical (top panels) and midlatitude winter (bottom panels) climates.

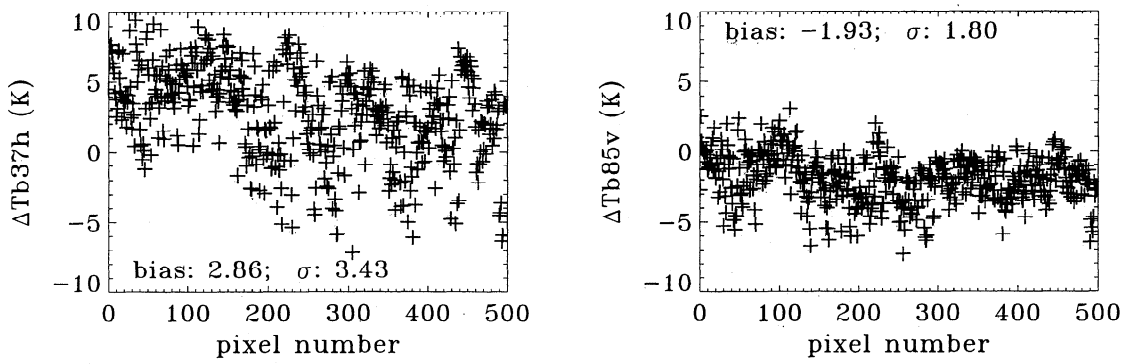

Figure 12. Brightness temperature differences (in units Klvin) between SSM/I measurements and simulations at 37h (left) and 85v (right) channels for clear-sky cases.

Because many factors affect Tb values for cloudy sky cases, we choose clear-sky data to test the differences between model results and microwave observations. Microwave data from SSM/I on the satellite of the Defense Meteorological Satellite Program, F-11, are used here. For this purpose, visible and infrared measurements from the Meteosat at 0° longitude are collocated with SSM/I data to within ±15 min. The Meteosat data were taken during the Atlantic Stratocumulus Transition Experiment (ASTEX) during July 1992 for a region of the Atlantic covering 25° to 40°N and 330° to 345°E. The bispectral threshold technique of *Minnis et al.* [1987, 1992] was used to retrieve cloud cover, optical thickness, cloud top temperature, and SST in each 0.5° grid box. Clear sky is defined, using the Meteosat analyses, as zero cloud cover within a grid box. This definition avoids cloud contamination produced by the low spatial resolution of the SSM/I. Near-sea-surface wind speeds are estimated from SSM/I data using the method defined by *Goodberlet et al.* [1990].

Given SST from Meteosat and WS from SSM/I, CWV is the major uncertainty in determining clear-sky brightness temperatures. In this case, 22 GHz Tb values are used as a baseline to intercalibrate model-simulated and SSM/I-observed brightness temperatures.

The model results and SSM/I measurements are compared as follows: (1) Simulate SSM/I Tb values according to the estimated SST and WS and a given minimal CWV value of 5 kg/m^2. (2) Compare model-simulated Tb with SSM/I observations for the 22-GHz channel. If the model Tb is less than the observation, increase CWV until the simulated 22v Tb is equal to the SSM/I-observed value. In this step, clear-sky CWV values are estimated as side products. (3) Check the differences in the observed and simulated Tb values for the 19-, 37-, and 85-GHz channels.

The advantage of this procedure is that the biases in the other channels, especially in the 37h and 85v channels used for LWP and Tw estimation, can be easily estimated. The disadvantage is that the absolute biases between the 22v channel and all other frequencies and polarizations are lost. In that sense, the current calibration is only relative and is specific to the particular radiative model and the SSM/I sensor.

Figure 12 gives the Tb difference between SSM/I observations and model simulations for 37h (left panel) and 85v (right panel) channels. The test gives biases for the 37h and 85v channels of about 2.86 K and -1.93 K, respectively. The biases in other channels are similar in magnitude. Although these values are relatively small (less than 2%), they are not negligible for physical retrievals (see section 3). *Greenwald et al.* [1993] found a similar bias of 3.58K for the SSM/I 37-GHz channels. Others [e.g., *Petty* 1990] also find small differences between model-simulated and SSM/I-observed Tb values at all SSM/I frequencies. These small biases could be produced by either uncertainties in the microwave radiative transfer models or by small errors in SSM/I instrument calibration.

Although we cannot estimate bias in the 22-GHz channel, we can estimate its direct effect by estimating CWV retrievals. Figure 13 compares the model CWV estimates with the values retrieved from the *Schluessel and Emery* [1990] scheme (hereinafter referred to as SE). The SE scheme is used because its retrievals were shown to have a high correlation coefficient (0.75) and small root-mean-square error (5.31 kg/m^2) when compared with radiosonde data [*Sheu and Liu*, 1995]. Our comparison shows that the current results are well correlated with the SE method (a correlation coefficient of about 0.98) with a relatively small bias of 4.39 kg/m^2. The linearity in Figure 13 is a result of the primary use of the 22-GHz channels in both the SE method and the current approach, as well as the fact that the 22-GHz channel is not saturated for water vapor levels typical of the ASTEX data.

In summary, clear-sky calibration tests suggest that the radiative model is consistent with the SSM/I observations. The differences between the two are small but not negligible

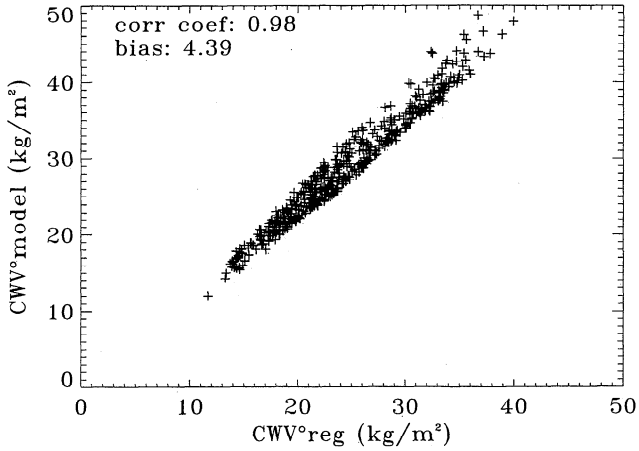

Figure 13. CWV (in units kg/m^2) comparison between the current model estimates and the retrievals using the *Schluessel and Emery* [1990]'s method.

for physical retrievals. Studies should be directed at further reducing these differences.

5. Summary

Simulated SSM/I brightness temperature values are significantly affected by both cloud water path and temperature and usually increase with increasing LWP for warm nonprecipitating clouds in oceanic environments. Unlike lower-frequency channels, the brightness temperatures at 85 GHz do not increase but decrease with decreasing cloud water temperature. The relationship between 85 GHz Tb and LWP is complicated by the fact that the brightness temperatures at this frequency can increase or decrease with increasing LWP depending on the difference (or competition) between Tw and the upwelling radiance at cloud base. It has been shown that the different dependencies of 37- and 85-GHz radiation on cloud temperature can be exploited to estimate LWP and Tw for liquid water clouds simultaneously using SSM/I brightness temperatures at those frequencies.

Sensitivity tests show that CWV uncertainties are the most important error source for Tb, LWP, and Tw estimation, while nonprecipitating ice clouds have little effect on SSM/I Tb values. Thus by combining microwave with IR remote sensing for nonprecipitating clouds, it should be possible to determine the cloud temperature for both an upper ice particle cloud layer using the IR sensor while simultaneously deriving cloud temperature and LWP for a lower liquid-water layer, even when optically thick ice clouds are present.

When all SSM/I instrument noise, SST, WS, and CWV error sources are considered, we find that the biases in cloud LWP estimates for current microwave methods are very small (within 0.01 mm), while standard deviations are about 0.02 - 0.04 mm depending on cloud temperature. The Tw bias and standard deviation decrease with increasing LWP from about 6 and 8 K for clouds with small LWP to less than 1 K for LWP > 0.4 mm. For most marine stratocumulus clouds (LWP ~ 0.1 to 0.2 mm) the Tw bias error is about 2 K and the standard deviation is 4 K. This result shows that cloud height estimated by using these microwave methods will have an uncertainty of about 1-2 km. While these errors may be relatively large compared to those for IR retrievals of cloud height for unobstructed low clouds, they represent a dramatic improvement for estimating the height of the lower cloud in overlapped conditions. Furthermore, the combined retrieval of Tw and LWP may reduce the error in LWP by about a factor of 2 because it could yield a temperature that is closer to the true cloud temperature than assumed in most microwave LWP retrievals.

Because of relatively strong water vapor absorption at 22 GHz, the brightness temperatures at this frequency are used to calibrate the radiative-model-simulated results and to estimate column water vapor. This relative calibration shows that there are small but not negligible differences between SSM/I observations and model simulations. By applying this calibration to each data set, it will be possible to apply the technique developed here to any SSM/I data set taken over ocean.

Acknowledgments. This research is part of the studies of the Clouds and the Earth's Radiant Energy System under the NASA Earth Observing System and the First ISCCP Regional Experiment. One of the authors (BL) gratefully acknowledges support from NASA under contract NAS1-19656. Some of the satellite data analyses were supported by the Office of Naval Research through R. F. Abbey under Grant USN-N0001491IMP24011. The DMSP data were provided by the Distributed Active Archive Center at the NASA Marshall Space Flight Center in Huntsville, Alabama. F. Wentz of Remote Sensing Systems in Santa Rosa, California supplied the algorithms for reducing SSM/I antenna temperatures. The 1992 Meteosat data were purchased from the European Space Agency with the assistance of Genevieve Seze of the Laboratoire Meteorologie Dynamique in Paris, France.

References

Baum, B.A., R.F. Arduini, B.A. Wielicki, P. Minnis, and S.C. Tsay, Multilevel cloud retrieval using multispectral HIRS and AVHRR data: nighttime oceanic analysis, *J. Geophys. Res., 99*, 5499-5514, 1994.

Charlock, T., F. Rose, T. Alberta, G. L. Smith, D. Rutan, N. Manalo-Smith, P. Minnis, and B. Wielicki, Cloud profiling radar requirements: Perspective from retrievals of the surface and atmospheric radiation budget and studies of atmospheric energetics, Utility and Feasibility of a Cloud Profiling Radar, *WCRP-84, IGPO Publ. Ser. 10*, pp, B10-B21, World Clim. Res. Program, Geneva, 1994.

Feigelson, E.M., Preliminary radiation model of a cloudy atmosphere, I, Structure of cloud and solar radiation, *Beitr. Phys. Atmos., 51*, 203-229, 1978.

Goodberlet, M.A., C.T. Swift, and J.C. Wilkerson, Ocean surface wind speed measurements of Special Sensor Microwave/Imager (SSM/I), *IEEE, GE-28*, 832-828, 1990.

Greenwald, T.J., G.L. Stephens, T.H. Vonder Haar, and D.L. Jackson, A physical retrieval of cloud liquid water over the global oceans using SSM/I observations, *J. Geophys. Res., 98*, 18,471-18,488, 1993.

Gupta, S.K., W.L. Darnell, and A.C. Wilber, A parameterization for surface longwave radiation from satellite data: Recent improvements, *J. Appl. Meteoolr., 31*, 1361-1367, 1992.

Hanh, C.J., S.G. Warren, J. Gordon, R.M. Chervin, and R. Jenne, Atlas of simultaneous occurrence of different cloud types over ocean, *NCAR Tech. Note TN-201 + STR*, 212 pp. Natl. Cent. for. Atmos. Res., Boulder, Colo., 1982.

Hanh, C.J., S.G. Warren, J. Gordon, R.M. Chervin, and R. Jenne, Atlas of simultaneous occurrence of different cloud types over land, *NCAR Tech. Note TN-241 + STR*, 211pp. Natl. Cent. for. Atmos. Res., Boulder, Colo., 1984.

Hobbs, P.V., and A.L. Rangno, Ice particle concentrations in clouds, *J. Atmos. Sci., 42*, 2523-2549, 1985.

Hollinger, J.P., J.L. Peirce, and A. Poe, SSM/I instrument evaluation, *IEEE, GE-28*, 781-790, 1990.

Li, Z., and H. Le Treut, Cloud radiation feedbacks in a general circulation model and their dependence on cloud modelling assumptions, *Clim. Dyn., 7*, 133-139, 1992.

Liao, X., W. Rossow, and D. Rind, Comparison betwen SAGE II and ISCCP high level clouds, 1, Global and zonal mean cloud amounts, *J. Geophys. Res., 100*, 1121-1135, 1995.

Liebe, H.J., An updated model for millimeter wave propagation in moist air, *Radio Sci., 20*, 1069-1089, 1985.

Liebe, H.J., G. Hufford, and T. Manabe, A model for the complex permittivity of water at frequencies below 1 THz, *Int. J. Infrared Millimeter Waves, 12*, 659-675, 1991.

Lin, B., Observations of cloud water path and precipitation over oceans using ISCCP and SSM/I data, Ph.D. dissertation, Dep. of Geol. Sci., Columbia Univ., New York, 1995.

Lin, B., and W.B. Rossow, Observations of cloud liquid water path over oceans: Optical and microwave remote sensing methods, *J. Geophys. Res., 99*, 20,907-20,927, 1994.

Lin, B., and W.B. Rossow, Seasonal variation of liquid and ice water path in non-precipitating clouds over oceans, *J. Clim.*, 9, 2890-2902, 1996.

Lin, B., and W.B. Rossow, Precipitation water path and rainfall rate estimates over oceans using special sensor microwave imager and International Satellite Cloud Climatology Project data, *J. Geophys. Res., 102*, 9359-9374, 1997.

Lin, B., P. Minnis, B. Wielicki, D. R. Doelling, R. Palikonda, D. F. Young, and T. Uttal, Estimation of water cloud properties from satellite microwave, infrared and visible measurements in oceanic environments. 2, Results, *J.Geophys. Res.*, this issue.

Liu, G., and J.A. Curry, Retrieval of precipitation from satellite microwave measurements using both emission and scattering, *J. Geophys. Res., 97*, 9959-9974, 1992.

Liu, G., and J.A. Curry, Determination of characteristic features of cloud liquid water from satellite microwave measurements, *J. Geophys. Res., 98*, 5069-5092, 1993.

McClathey, R.A., R.W. Fenn, J.E.A. Selby, F.E. Voltz, and J.S. Garing, Optical properties of the atmosphere, *AFCRL-72-0497, Environ. Res. Pap., 411*, Air Force Cambridge Res. Lab., Cambridge, Mass., 1972.

Minnis, P., E. Harrison, and G. Gibson, Cloud cover over the equatorial eastern Pacific derived from July 1983 International Satellite Cloud Climatology Project data using a hybrid bispectral threshold method, *J. Geophys. Rev., 92*, 4051-4073, 1987.

Minnis, P., P.W. Heck, D.F. Young, C.W. Fairall, and J.B. Snider, Stratocumulus cloud properties derived from simultaneous satellite and island-based instrumentation during FIRE, *J. Appl. Meteorol., 31*, 317-339, 1992.

Minnis, P., P.W. Heck, and D.F. Young, Inference of cirrus cloud properties using satellite-observed visible and infrared radiances, II, Verification of theoretical cirrus radiative properties, *J. Atmos. Sci., 50*, 1305-1322, 1993.

Pandey, C.P., E.G. Njoku, and J.W. Waters, Inference of cloud temperature and thickness by microwave radiometery from space, *J. Clim. Appl. Meteorol., 22*, 1894-1898, 1983.

Petty, G.W., On the response of the special sensor microwave/imager to the marine environment--Implications for atmospheric parameter retrievals, Ph.D. dissertation, Dep. of Atmos. Sci., Univ. of Wash., Seattle, 1990.

Petty,. G.W., and K.B. Katsaros, The response of the SSM/I to the marine environment, I, An analytic model for the atmospheric component of observed brightness temperatures, *J. Atmos. Oceanic Technol., 9*, 746-761, 1992.

Petty,. G.W., and K.B. Katsaros, The response of the SSM/I to the marine environment, II, A parameterization of the effect of the sea surface slope distribution on emission and reflection, *J. Atmos. Oceanic Technol., 11*, 617-628, 1994.

Poore, K., J. Wang, and W.B. Rossow, Cloud layer thicknesses from a combination of surface and upper-air observations, *J. Clim., 8*, 550-568, 1995.

Ramanathan, V., R.D. Cess, E.F. Harrison, P. Minnis, B.R. Barkstrom, E. Ahmad and D. Hartmann, Cloud radiative forcing and climate: results from the Earth Radiation Budget Experiment, *Science, 243*, 57-63, 1989.

Ray, P.S., Broadband complex refractive indices of ice and water, *Appl. Opt., 11*, 1836-1844, 1972.

Rossow, W.B., and L.C. Garder, Validation of ISCCP cloud detections, *J. Clim., 12*, 2370-2393, 1993.

Rossow, W.B., and A. Lacis, Global, seasonal cloud variations from satellite radiance measurements, II, Cloud properties and radiative effects, *J. Clim., 3*, 1204-1253 1990.

Rossow, W.B., and Y.C. Zhang, Calculation of surface and top of atmosphere radiative fluxes from physical quantities based on ISCCP data sets, 2, Validation and first results, *J. Geophys. Res., 100*, 1167-1197, 1995.

Sassen, K., D. Starr, and T. Uttal, Mesoscale and microscale structure of cirrus clouds: Three case studies, *J. Atmos. Sci., 46*, 371-396, 1989.

Schluessel, P., and W.J. Emery, Atmospheric water vapor over oceans from SSM/I measurements, *Int. J. Remote Sens., 11*, 753-766, 1990.

Sheu, R.-S., and G. Liu, Atmospheric humidity variations associated with westerly wind bursts during TOGA COARE, *J. Geophys. Res., 100*, 25,759-25,768, 1995.

Smith E., A. Mugnai, H. Cooper, G. Tripoli, and X. Xiang, Foundations for statistical-physical precipitating retrieval from passive microwave satellite measurements, I, Brightness temperature properties of a time dependent cloud-radiation model, *J. Appl. Meteorol., 31*, 506-531, 1992.

Tian, L., and J.A. Curry, Cloud overlap statistics, *J. Geophys. Res., 94*, 9925-9935, 1989.

Warren, S.G., Optical constants of ice from the ultraviolet to the microwave, *Appl. Opt., 23*, 1206-1255, 1984.

Warren, S.G., C.J. Hanh, and J. London, Simultaneous occurrence of different cloud types, *J. Clim. Appl. Meteorol., 24*, 658-667, 1985.

Warren, S.G., C.J. Hanh, J. London, R.M. Chervin, and R.L. Jenne, Global distribution of total cloud cover and cloud type amounts over ocean, *NCAR Tech. Note, NCAR/TN-317+STR*, 42 pp., plus 170 maps, Natl. Cent. for Atmos. Res., Boulder, Cplo., 1988.

Wielicki, B.A., R.D. Cess, M.D. King, D.A. Randall, and E.F. Harrison, Mission to planet earth: Role of clouds and radiation in climate, *Bull. Am. Meteorol. Soc., 76*, 2125-2153, 1995.

Wilheit, T.T., A.T.C. Chang, M.S.V. Rao, E.B. Rodgers, and J.S. Theon, A satellite technique for quantitatively mapping rainfall rates over the oceans, *J. Appl. Meteorol., 16*, 551-560, 1977.

Yeh, H.-Y.M., N. Prasad, R.A. Mack, and R.F. Adler, Aircraft microwave observations and simulations of deep convection from 18 to 183 GHz, II, Model results, *J. Atmos. Oceanic Technol., 7*, 392-410, 1990.

B. Lin, B. Wielicki, and P. Minnis, Mail Stop 420, NASA Langley Research Center, Hampton, VA 23681-0001. (e-mail: bing@front.larc.nasa.gov)

W. B. Rossow, NASA Goddard Institute for Space Studies, 2880 Broadway, New York, NY 10025. (e-mail: clwbr@giss.nasa.gov)

(Received June 11, 1997; revised September 30, 1997; accepted October 2, 1997.)